Available online at www.sciencedirect.com
ScienceDirect
Journal of the European Ceramic Society 26 (2006) 3467–3475
www.elsevier.com/locate/jeurceramsoc

Effect of post-sintering heat-treatment on thermal and mechanical properties of Si_3N_4 ceramics sintered with different additives

Thanakorn Wasanapiarnpong [a,*], Shigetaka Wada [b], Masamitsu Imai [a], Toyohiko Yano [a]

[a] *Research Laboratory for Nuclear Reactors, Tokyo Institute of Technology, 2-12-1 O-okayama, Meguro, Tokyo 152-8550, Japan*
[b] *Department of Material Science, Faculty of Science, Chulalongkorn University, Bangkok 10330, Thailand*

Received 20 May 2005; received in revised form 25 October 2005; accepted 29 October 2005
Available online 20 December 2005

Abstract

To improve the thermal conductivity of Si_3N_4 ceramics, elimination of grain-boundary glassy phase by post-sintering heat-treatment was examined. Si_3N_4 ceramics containing SiO_2–MgO–Y_2O_3-additives were sintered at 2123 K for 2 h under a nitrogen gas pressure of 1.0 MPa. After sintering, the SiO_2 and MgO could be eliminated from the ceramics by vaporization during post-sintering heat-treatment at 2223 K for 8 h under a nitrogen gas pressure of 1.0 MPa. Thermal conductivity of 3 mass% SiO_2, 3 mass% MgO and 1 mass% Y_2O_3-added Si_3N_4 ceramics increases from 44 to 89 $Wm^{-1} K^{-1}$ by the decrease in glassy phase and lattice oxygen after the heat-treatment. Relatively higher fracture toughness (3.8 MPa $m^{1/2}$) and bending strength (675 MPa) with high hardness (19.2 GPa) after the heat-treatment were achieved in this specimen. Effects of heat-treatment on microstructure and chemical composition were also observed, and compared with those of Y_2O_3–SiO_2-added and Y_2O_3–Al_2O_3-added Si_3N_4 ceramics.

Keywords: Thermal conductivity; Si_3N_4; Mechanical properties

1. Introduction

Ceramic substrates are used widely for electrical circuits due to their high thermal conductivity, high electrical resistivity, and high mechanical strength. Alumina substrate is most popular. Thermal conductivity of polycrystalline alumina is around 25–35 $Wm^{-1} K^{-1}$ and up to 40 $Wm^{-1} K^{-1}$ for single crystal.[1] Beryllium oxide (BeO) substrates have been used for high power electronic application because of their superior thermal conductivity around 240 $Wm^{-1} K^{-1}$. By now, beryllium oxide has lost its popularity because of the safety controversy. Aluminum nitride (AlN) substrates are replacing the BeO in numerous applications. Aluminum nitride substrates are more expensive than alumina substrates. But they have thermal conductivity of 175–200 $Wm^{-1} K^{-1}$ and are toxic free.[1]

Silicon nitride (Si_3N_4) ceramic substrates have been interesting for electrical substrate applications, because Si_3N_4 has high intrinsic thermal conductivity. Hirosaki et al.[2] reported that the intrinsic thermal conductivity of single crystal β-Si_3N_4 is 450 $Wm^{-1} K^{-1}$, while the intrinsic thermal conductivity of single crystal AlN is 320 $Wm^{-1} K^{-1}$. Moreover, bending strength of Si_3N_4 (600–1500 MPa) is higher than that of AlN (300–350 MPa).[3] Akimune et al.[4] reported the highest thermal conductivity of 162 $Wm^{-1} K^{-1}$ for 0.5 mol% Y_2O_3 and 0.5 mol% Nd_2O_3-added Si_3N_4 ceramics fabricated by hot isostatic pressing (HIP) at 2473 K. Kitayama et al.[5] fabricated Y_2O_3–SiO_2-added Si_3N_4 by hot pressing at 2073 K, 40 MPa, 2 h. Subsequently, by the heat-treatment at 2123 K for 4 h under 1.0 MPa of nitrogen atmosphere, the thermal conductivity of the ceramic along the hot pressing axis was reported to be 79 $Wm^{-1} K^{-1}$.

Hot-isostatic pressing and hot pressing process is not so suitable for mass production of ceramic substrates. Generally, relatively large amount of additives are required to obtain dense Si_3N_4 ceramics, not only pressureless sintering and gas-pressure sintering but also sintering under applied pressure. During sintering, additives react with SiO_2 (including surface oxide of a Si_3N_4 raw powder) to form a liquid phase. Most of liquid phase

* Corresponding author. Tel.: +81 3 5734 3082; fax: +81 3 5734 2859.
E-mail address: thanakorn@nr.titech.ac.jp (T. Wasanapiarnpong).

0955-2219/$ – see front matter © 2005 Elsevier Ltd. All rights reserved.
doi:10.1016/j.jeurceramsoc.2005.10.011

changed into non-crystalline solid (glassy phase) during cooling down. The role of liquidus phase is promoting densification of ceramics, leading to higher thermal conductivity due to elimination of porosity. On the other hand, smaller amount of glassy phase is promising within the Si_3N_4 ceramics having almost full density. Generally, during sintering stage excess amount of glassy phase is usually applied for easier densification. Thus, obtained dense Si_3N_4 usually contains relatively large amount of additives. Therefore, the sintered Si_3N_4 ceramics have generally low thermal conductivity (20–40 $Wm^{-1} K^{-1}$) due to the presence of this glassy phase, which has poor thermal conductivity (≈1 $Wm^{-1} K^{-1}$).[3]

Hirosaki et al.[6] reported that high thermal conductivity was established by growth of Si_3N_4 grains. However, large grain size usually leads to poor mechanical properties. The comparison of thermal conductivity and mechanical properties, affected by grain growth, have not been reported.

In this study, Si_3N_4 ceramics were fabricated by gas pressure sintering. Yttrium oxide (Y_2O_3), silica (SiO_2), alumina (Al_2O_3) and magnesia (MgO) were used for liquid-phase-enhanced sintering process. Dense materials were sintered by this process, but their thermal conductivities were not so high (30–40 $Wm^{-1} K^{-1}$). Therefore, post-sintering heat-treatment process was performed to reduce excess amount of glassy phase. During the heat-treatment, chemical reactions between Si_3N_4 and SiO_2, Al_2O_3 or MgO may generate SiO, N_2 and Mg-gas according to the following reactions at 2200 K under 1 atm[7];

$$Si_3N_4(s) + 3SiO_2(l) \rightarrow 6SiO(g) + 2N_2(g) \quad (\Delta G^\circ = -77.748\,kJ/mol) \tag{1}$$

$$Si_3N_4(s) + Al_2O_3(s) \rightarrow 3SiO(g) + 2AlN(s) + N_2(g) \quad (\Delta G^\circ = +8.651\,kJ/mol) \tag{2}$$

$$Si_3N_4(s) + 3MgO(s) \rightarrow 3SiO(g) + 3Mg(g) + 2N_2(g) \quad (\Delta G^\circ = +20.490\,kJ/mol) \tag{3}$$

In the previous study,[8] it is clarified that the reaction (1) was promoted to reduce the amount of glassy phase in the Y_2O_3–SiO_2-added Si_3N_4 due to post-sintering heat-treatment, and thermal conductivity of the ceramic improved to 84 $Wm^{-1} K^{-1}$. In the case of Y_2O_3–Al_2O_3-added Si_3N_4, the effect of post-sintering heat-treatment was not so significant. This indicated that the effect of sintering aids depended not only amount but also the kind of additives.

In this work, the effects of post-sintering heat-treatment on oxygen content, weight and density change, thermal conductivity and chemical composition of Si_3N_4 ceramics containing silica, magnesia and yttria have been explored to confirm the above-mentioned mechanism, and it is aimed to obtain high thermal conductivity Si_3N_4 without HIP or hot-press process. Furthermore, the effects of post-sintering heat-treatment on mechanical properties and microstructure of not only Si_3N_4 containing silica, magnesia and yttria but also Si_3N_4 containing yttria and silica or yttria and alumina specimens were observed to clarify the effects of the post-sintering heat-treatment on thermal and mechanical properties.

2. Experimental procedure

Si_3N_4 ceramics were prepared from a high-purity α-Si_3N_4 raw powder (particle size 0.8 μm, oxygen content 1.3 mass%; SN-E10 grade, Ube Industries, Japan) with Y_2O_3 (RU, Shin-Etsu Chemical, Japan), SiO_2 (KE-P30, Nippon Shokubai, Japan), Al_2O_3 (TMD, Taimei Chemical, Japan) and MgO (surface area 31.7 m^2/g, Iwatani Chemicals, Japan) as sintering aids. Weight ratios of starting composition were Si_3N_4:Y_2O_3:SiO_2 = 92:5:3 (5Y3S), Si_3N_4:Y_2O_3:Al_2O_3 = 92:5:3 (5Y3A) and Si_3N_4:SiO_2:MgO:Y_2O_3 = 93:3:3:1 (3S3M1Y). Mixtures were ball-milled for 24 h in a polyethylene bottle with silicon nitride balls (SN-12, diameter 5 mm, Nikkato Corporation, Japan) and ethanol (99.5%) as a medium. Slurries were dried in a rotary evaporator at a temperature of 333 K and the mixed powder was sieved through a 100-mesh sieve. Approximately 0.5 g of the dried powder was uniaxially pressed under 20 MPa in a die of 13 mm in diameter. The pellet was then isostatically cold-pressed (CIP) under a pressure of 200 MPa. CIPed pellets were placed in a BN crucible filled with a powder mixture of 50 mass% Si_3N_4 and 50 mass% BN as a packing powder and placed in a larger carbon crucible. Samples were sintered in a graphite furnace (High-Multi 5000, Fuji Dempa Ltd., Japan) at 2123 K for 2 h under a nitrogen pressure of 1.0 MPa.

Post-sintering heat-treatment process to remove grain-boundary glassy phases was performed by re-firing the sintered bodies at 2073–2223 K for 8 h under a nitrogen pressure of 1.0 MPa without a packing powder using the same furnace used to sintering. The density of sintered and heat-treated specimens was measured by the Archimedes method using water.

Sintered and heat-treated specimens were ground in a SiC mortar and sieved through a 200-mesh sieve for phase identification and oxygen/nitrogen content determination. Phase identification and lattice parameter determination were performed by X-ray diffractometry (XRD, PW 1700, Philips, Holland).

A commercial hot-gas-extraction analyzer (TC-436, LECO Co.) was used for oxygen and nitrogen concentration analysis. About 20 mg of each powder sample was weighed into a graphite crucible (10 mm inner diameter × 16 mm height), and about 50 mg of graphite powder was added to the sample to accelerate the carbo-thermal reduction of oxide phases. The crucible was heated up to 2500 K within 400 s in a flowing helium atmosphere. The total amount of oxygen and nitrogen released from the powder as a function of temperature was recorded, and was corrected using standards. Three measurements were performed for all samples and the average is used as the measured value. Amount of oxygen distributed in Si_3N_4 lattice (lattice oxygen) was approximated by Gaussian peak separation of the evolution curve during heating after Kitayama et al.[9] using the HF-treated powders (46% HF, 3 h at 333 K and 50% H_2SO_4, 6 h at 373 K).

Specimens for measuring thermal conductivity were finished using a diamond wheel subsequently by 1 μm diamond slurry for smooth and parallel surfaces. Thermal conductivity of the polished specimens was measured at room temperature by laser flash method (LF/TCM, FA 8510B, Rigaku, Japan). After the thermal conductivity measurement, specimens were re-polished using 1 μm diamond slurry, plasma-etched in CF_4/O_2 gas, coated with evaporated carbon, and observed by a field-emission scanning electron microscope (FE-SEM, S-4800, Hitachi, Japan). Average grain size was determined from secondary electron images using the linear-intercept method. Back-scattered electron-images were used for illuminating intergranular glassy phase, and the amount of grain-boundary phase was estimated using the image analysis program (WinROOF 5.03, Mitani, Japan). The area appearing bright in the back-scattered electron-image was supposed to contain yttrium, which localized mainly in the intergranular phase. Five images (19 μm × 25 μm) for each sample were taken as digital data for analysis. Yttrium, aluminum and magnesium contents were measured from polished and carbon-coated surface of each specimen by WDX (Wave length Dispersive X-ray spectroscopy, WDX400, Oxford Instruments, USA) using standards.

For the bending strength measurement, samples were prepared from approximately 8.5 g of the dried powder, uniaxially pressed under 20 MPa in a square die of 35 mm and subsequently isostatically cold-pressed under a pressure of 200 MPa. Samples were sintered and post-sintering heat-treated by the same condition as mentioned above. Rectangular bars 3 × 4 × 25 mm were cut and ground by 1 μm diamond slurry. Mechanical testing was performed using the commercial screw-driven load frame (Instron, Model 1185, Canton, USA) with a 3-point bend fixture. Test conditions were as follows; loading with 20-mm span and a crosshead speed of 0.5 mm/min in air at room temperature. Young's modulus was calculated from the stress–strain curve of 3-point bending test with 2 mm strain gage (Kyowa, Japan) attached on the tensile surface of the specimen. Fracture surfaces were observed by the FE-SEM.

Vickers hardness was measured using a Vickers hardness tester at room temperature (Hardness tester AVK-A, Akashi, Japan). The load and loading time were 5 kgf and 15 s, respectively. Fracture toughness was deduced from the diagonal length and crack length of Vickers indentations according to JIS R 1607.

3. Results and discussion

3.1. Thermal properties

Table 1 summarizes the variation of density, mass loss, total oxygen content, lattice parameter, thermal diffusivity, and thermal conductivity of the 3S3M1Y specimen after sintering at 2123 K for 2 h and after the post-sintering heat-treatment at 2223 K for 8 h. The data for the 5Y3S and 5Y3A specimens referred from the previous paper are also listed for comparison.[8]

All specimens could be sintered to higher than 95% of theoretical density and did not so much change after the heat-treatment at 2223 K for 8 h. Image analysis conducted on polished cross sections of these specimens revealed that there was no porous layer in all heat-treated specimens. It should indicate that the mass loss during the heat-treatment occurred through diffusion of substances from bulk to surface and vaporization from the surface of specimens.

Fig. 1 shows mass loss occurred during the heat-treatment of the 3S3M1Y specimen compared with those of 5Y3S, 5Y3A specimens.[8] The mass loss of the 3S3M1Y specimen was

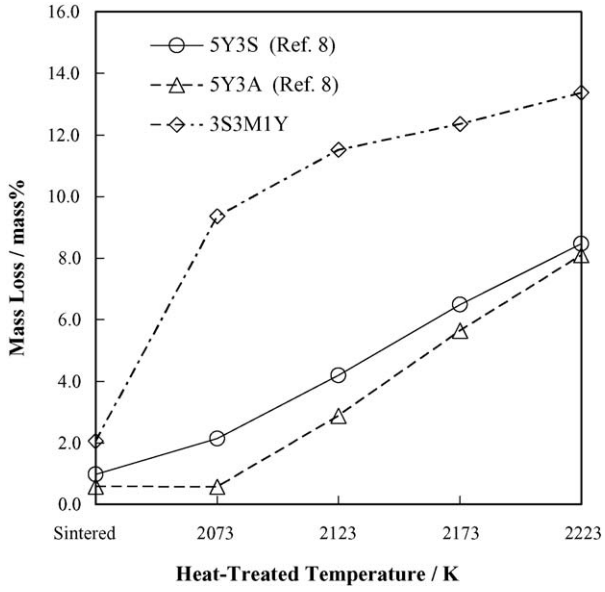

Fig. 1. Effect of heat-treatment temperature on mass loss of 5Y3S, 5Y3A and 3S3M1Y-added Si_3N_4 ceramics sintered at 2123 K for 2 h under a nitrogen gas pressure of 1.0 MPa and subsequently heat-treated at 2073–2223 K for 8 h under a nitrogen gas pressure of 1.0 MPa.

Table 1
Bulk density, mass loss, oxygen content, lattice parameter, thermal diffusivity and thermal conductivity of the Si_3N_4 ceramics sintered at 2123 K for 2 h (left column) and after the heat-treated at 2223 K for 8 h (right column)

Formula	Bulk density (g/cm^3)	Mass loss (mass%)	Oxygen content (mass%)	Lattice parameter		Thermal diffusivity (cm^2/s)	Thermal conductivity ($Wm^{-1}\,K^{-1}$)
				a (pm)	*c* (pm)		
5Y3S[a]	3.18/3.27	0.97/8.46	3.05/0.99	760.19/760.17	290.63/290.71	0.167/0.370	37.1/84.4
5Y3A[a]	3.27/3.23	0.58/8.09	3.17/1.24	760.34/760.33	290.95/291.00	0.127/0.157	29.1/35.1
3S3M1Y	3.18/3.16	2.06/13.4	3.23/0.46	760.21/760.03	290.89/290.90	0.193/0.400	43.9/89.3
Accuracy	±0.01	±0.01	±0.05	±0.05	±0.05	±0.002	±0.1

[a] Reprinted from Ref. 8.

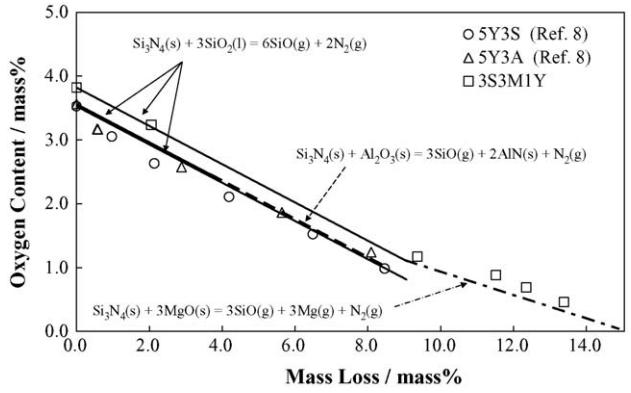

Fig. 2. Relationship between mass loss and oxygen content of 5Y3S, 5Y3A and 3S3M1Y-added Si_3N_4 ceramics during heat-treatment. Solid line, dashed-line and centered-line represent the estimated oxygen content calculated by mass loss reaction of Eqs (1)–(3), respectively.

always larger than that of the 5Y3S and 5Y3A specimens, and increased with increasing heat-treatment temperature from 2073 to 2223 K. The trend of 5Y3S specimen was almost the same as that of 5Y3A specimen. They showed the mass loss, which increased as a function of the heat-treatment temperature of more than 2123 K, but almost no change at 2073 K. Whereas, the mass loss of 3S3M1Y was very large at 2073 K, but slightly changed at more than 2123 K. The largest mass loss was found in the 3S3M1Y composition since it contained the highest amount of volatile species (SiO_2 and MgO). The mass loss found in all specimens would be due to the reaction of Si_3N_4 with additives and/or SiO_2 existed on the surface of the Si_3N_4 powder according to the chemical reactions (1)–(3), as mentioned before.[8]

Fig. 2 shows the relationship between mass loss and oxygen content of the 3S3M1Y specimen, and those of 5Y3S and 5Y3A specimens were reproduced from the previous paper.[8] These graphs contained all data for all specimens after heat-treatment at different temperatures. The data plotted at 0% mass loss corresponded to the oxygen content of the raw powder mixtures of each specimen. The relation between mass loss and oxygen content was supposed to indicate the chemical reaction occurred during the heat-treatment, such as the reactions (1)–(3). The SiO, N_2 and Mg gas should be generated during the heat-treatment at high temperature. The evaporation of SiO gas leads to the decrease of oxygen content of ceramic bodies.

Solid lines shown in Fig. 2 represent the mass loss relation calculated from the reaction (1). Comparing with the calculated data and observed data, the oxygen content data collected from the heat-treated specimens were very close to the calculated one for every series of specimens sintered with different additives. This result confirms the mass loss by the reaction (1).[8] Dashed line in Fig. 2 represents the mass loss relation calculated from the reaction (2). The oxygen content data collected from the specimens were also close to the calculated data by the Eq. (2). The mass loss in the 5Y3A specimen due to the reaction (2) was considered to have happened after the reaction (1) because the free energy change of the reaction (1) was lower than that of the reaction (2).[8] Centered line in Fig. 2 represents the mass loss relation calculated from the reaction (3). The oxygen content data collected from the specimen was also close to the calculated data by the reaction (3). The mass loss in the 3S3M1Y specimen due to the reaction (3) was considered to have happened after the reaction (1) because the free energy change of the reaction (1) was lower than that of the reaction (3), as in the case of the reaction (2). The highest mass loss (13.4%) found in the 3S3M1Y specimen led to the lowest total oxygen content (∼0.5%) without porous layer.

The change in average amount of yttrium, aluminum and magnesium due to the heat-treatment at 2223 K for 8 h of all specimens is shown in Table 2. Whereas, magnesium almost disappeared in the 3S3M1Y specimen, the amount of yttrium and aluminum in the other specimens did not change significantly by the heat-treatment. It supported that only SiO, N_2 and Mg-gas were generated during the heat-treatment according to the reactions (1)–(3).

However, the sequence of the mass loss reactions (1)–(3) cannot be considered only by the thermochemical data (Gibb's free energy). To confirm the kinetic of the chemical reactions, the change in average amount of yttrium and magnesium due to the mass loss reactions of the 3S3M1Y specimen is shown in Fig. 3. Zero percent of mass loss represents the concentration calculated from a raw powder. Slope of decreasing in magnesium content by mass loss reaction at initial part is low, but dramatically increases at higher amount of mass loss more than 10%. The result confirm that magnesium loss by the reaction (3) is also generated but the mass loss reaction is dominated by the reaction (1) at the initial part, whereas the mass loss is dominated by the reaction (3) in the final part.

In addition to the change in average amount of magnesium, yttrium content of the 3S3M1Y specimen did not change significantly at the wide range of mass loss. The amount of yttrium slightly increases probably due to the decreasing in the other elements, such as Si, Mg and O.

The effect of heat-treatment temperature on the thermal conductivity of sintered bodies is shown in Fig. 4. The 3S3M1Y specimen showed significant increase in thermal conductivity

Table 2
Chemical composition (mass%) of Si_3N_4 ceramics sintered at 2123 K for 2 h and after heat-treated at 2223 K for 8 h measured by WDX analysis

Element	5Y3S		5Y3A		3S3M1Y	
	Sintered	Heat-treated	Sintered	Heat-treated	Sintered	Heat-treated
Yttrium (Y)	3.60 (0.27)	3.28 (0.16)	3.54 (0.26)	3.73 (0.09)	0.68 (0.06)	0.89 (0.07)
Aluminium (Al)	–	–	1.71 (0.10)	1.65 (0.06)	–	–
Magnesium (Mg)	–	–	–	–	1.79 (0.05)	0.07 (0.01)

The values in parenthesis are standard deviation.

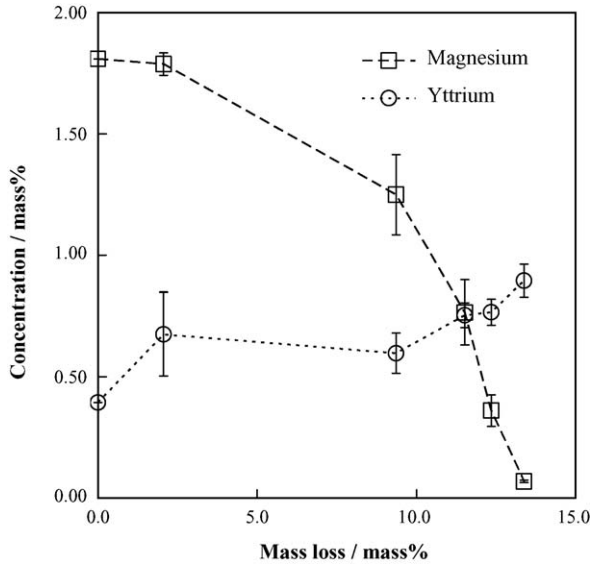

Fig. 3. Effect of mass loss reaction on the concentration of magnesium and yttrium during heat-treatment process of the 3S3M1Y specimen.

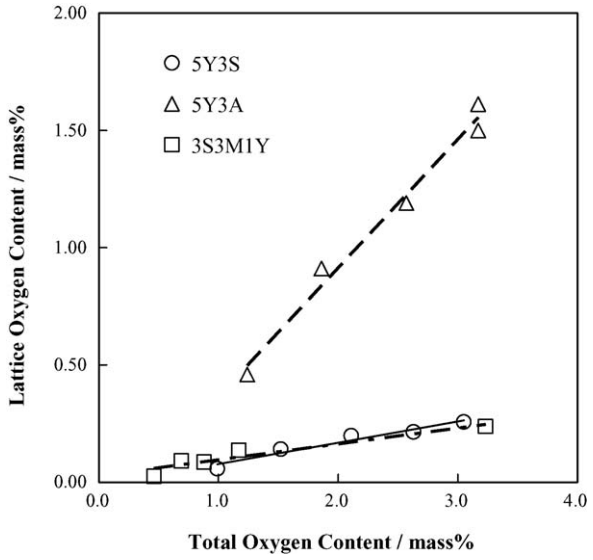

Fig. 5. Relationship between total oxygen content and lattice oxygen content of Si_3N_4 ceramics sintered at 2123 K for 2 h and heat-treated at 2073–2223 K for 8 h both under a nitrogen gas pressure of 1.0 MPa.

with increasing heat-treatment temperature as in the case of the 5Y3S specimen.[8] Thermal conductivity of the 5Y3S and the 3S3M1Y specimens increased more than 2 times (from 37 to 84 and 44 to 89 $Wm^{-1}\,K^{-1}$, respectively) after the heat-treatment at 2223 K for 8 h under a nitrogen gas pressure of 1.0 MPa. Thermal conductivity of the 5Y3S was always slightly lower than that of the 3S3M1Y specimen. On the other hand, thermal conductivity of the 5Y3A specimen was relatively low and not significantly increased with increasing heat-treatment temperature.[8]

Fig. 5 shows the relationship between total oxygen content and lattice oxygen content obtained from the profile analysis of the evolved oxygen during carbo-thermal hot gas extraction. The lattice oxygen content of all specimens decreased almost linearly with decreasing the total oxygen content. In other words, the lattice oxygen content decreased with increasing the heat-treatment temperature. As a result, the thermal conductivity of specimens increased and a high thermal conductivity of about 89 $Wm^{-1}\,K^{-1}$ could be achieved in the 3S3M1Y specimen heat-treated at 2223 K for 8 h with the lowest lattice oxygen content (0.03 mass%). The lattice oxygen content of the 5Y3A specimen was extensively higher than these of the other two specimens. Large amount of the lattice oxygen content only in the 5Y3A specimen was explained as a result of SiAlON formation. Nearly half amount of oxygen was included into lattice in this system. On the other hand, the lattice oxygen content of the 5Y3S and 3S3M1Y specimens was almost the same value and slope. Only about one tenth of oxygen was assigned as lattice oxygen. This result agreed with the same tendency of thermal conductivity on the heat-treatment temperature as shown in Fig. 4.

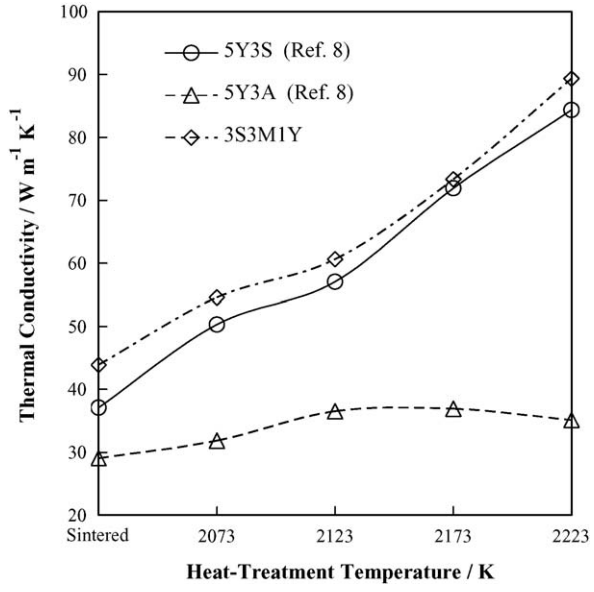

Fig. 4. Effect of heat-treatment temperature on thermal conductivity of Si_3N_4 ceramics sintered at 2123 K for 2 h and heat-treated at 2073–2223 K for 8 h both under a nitrogen gas pressure of 1.0 MPa.

Fig. 6a shows the relationship between total oxygen content and thermal conductivity of the ceramics, and Fig. 6b shows the relationship between lattice oxygen content and thermal conductivity of the ceramics. The data for the 5Y3S and 5Y3A specimens in Fig. 6a were referred from the previous report.[8] Thermal conductivity of the 5Y3S and 3S3M1Y specimens remarkably increased as the decrease of total oxygen content as same as lattice oxygen content. Comparing with the same amount of total oxygen content, Fig. 6a, the thermal conductivities of the 5Y3S specimen were almost higher than that of the 3S3M1Y specimen. On the other hand, the relationship between thermal conductivity and lattice oxygen content of the 5Y3S specimen was similar to that of the 3S3M1Y specimen. Comparing the effect of lattice oxygen content in crystalline phase to thermal conductivity of sintered bodies of the 5Y3S and 3S3M1Y specimens (Fig. 6b), they showed very similar tendency, whereas their total oxygen contents at the same conductivity showed 0.5–1.0% difference (Fig. 6a). Therefore,

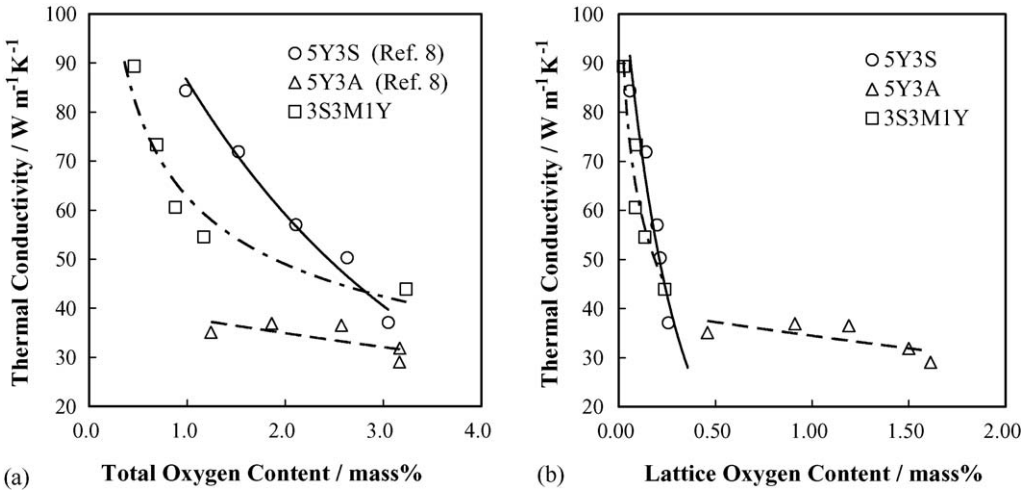

Fig. 6. Relationship between (a) total oxygen content, (b) lattice oxygen content and thermal conductivity of Si_3N_4 ceramics sintered at 2123 K for 2 h and heat-treated at 2073–2223 K for 8 h both under a nitrogen gas pressure of 1.0 MPa.

about 0.5 mass% of grain-boundary oxygen, i.e. difference in total oxygen content and lattice oxygen content, of these specimens does not so large effects on thermal conductivity of the ceramics. On the other hand, thermal conductivity of the 5Y3A specimen was not changed significantly in spite of large decrease in the total oxygen content and lattice oxygen content.

The poor thermal conductivity in Al_2O_3-added Si_3N_4 ceramics has been explained as a result of oxygen substitution for nitrogen incorporated with Al substitution for Si (β-SiAlON formation), therefore an amount of lattice oxygen increases in the case of Al_2O_3-added Si_3N_4. Thus thermal conductivity of crystal (grain) is restricted.[8,10–12] From Fig. 6b, the amount of lattice oxygen in the 5Y3A specimen is also reduced to ~0.46 mass% after the heat-treatment. However, the amount of lattice oxygen in the 5Y3A specimen is still greater than the cases of the 5Y3S or 3S3M1Y specimens. Therefore, it is confirmed that the amount of lattice oxygen should be a primary reason of the poor thermal conductivity of the 5Y3A specimen. Furthermore, it is noted that thermal diffusivity of only the 5Y3A specimen was not so greatly improved by the heat-treatment compared with the other specimens (Table 1). The thermal diffusivity of β-SiAlON was reported[12] to be 0.07 cm^2/s, which corresponds about one half of that of the 5Y3A specimen. This result also supports SiAlON formation in this specimen during sintering and SiAlON does not change into silicon nitride due to the heat-treatment.

X-ray diffraction (XRD) patterns of the sintered and the heat-treated samples are shown in Fig. 7. There is only β-Si_3N_4 crystalline phase observed in the sintered specimens. In addition to the glassy phase (Y–Si–O–N or Y–Si–Al–O–N), a slight amount of the high yttrium-containing oxynitride crystalline phase ($Y_4Si_2O_7N_2$) formed after the heat-treatment as a grain-boundary phase in the 5Y3S and 5Y3A specimens. On the other hand, there is no any secondary crystalline phase in the 3S3M1Y specimen neither as-sintered nor heat-treated.

Back-scattered electron micrographs of polished surfaces were observed by field emission scanning electron microscope (FE-SEM) as shown in Fig. 8. The area appearing bright in the back-scattered electron images was supposed to contain yttrium which localized in the intergranular phase. Fig. 8 illustrates the microstructure change by heat-treatment such as grain size, glassy pocket at triple or multi junction and glassy film between grains. By the heat-treatment, the volume percent of glassy phase decreased as the mass loss increased by the evaporation of gases as shown in Table 3.

As mentioned that the glassy phase has very low thermal conductivity compared to the Si_3N_4 grain. The decreasing in amount of glassy phase is one of several keys to get a high thermal conductivity ceramic materials. The distribution of glassy phase,

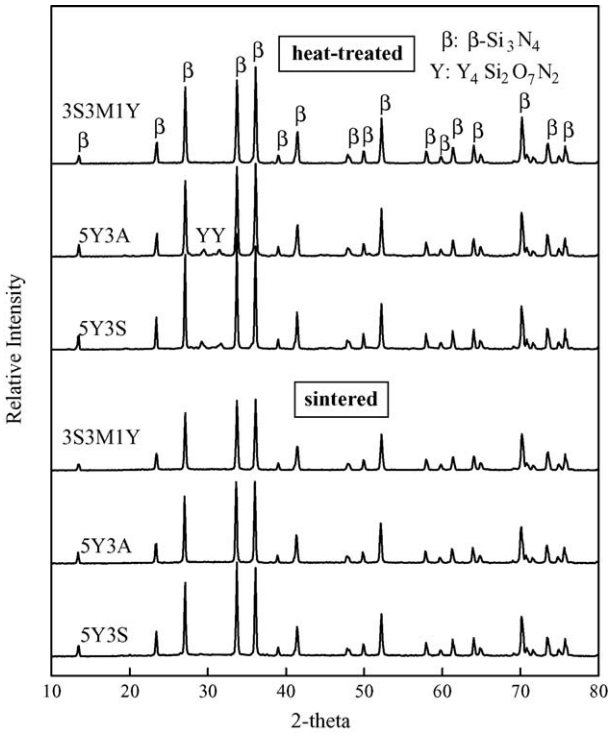

Fig. 7. XRD spectra of specimens sintered at 2123 K for 2 h and heat-treated at 2223 K for 8 h both under a nitrogen gas pressure of 1.0 MPa.

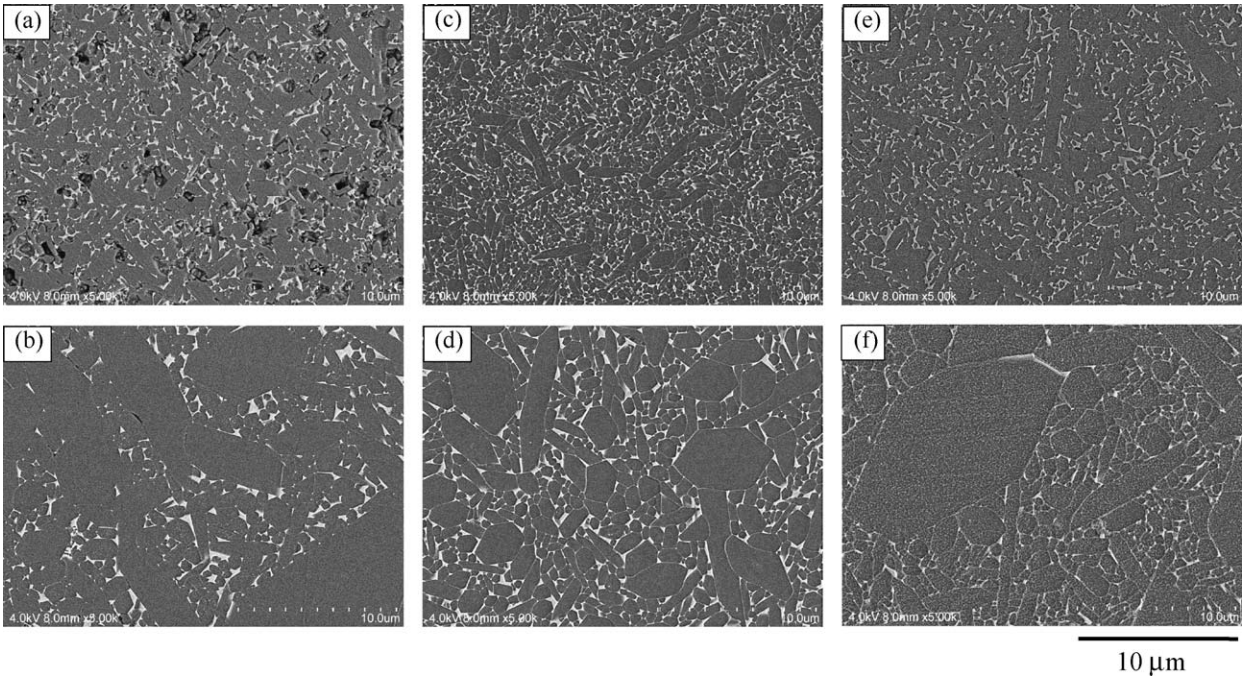

Fig. 8. Back-scattered electron micrographs of polished and plasma-etched surface of the Si_3N_4 ceramics sintered at 2123 K for 2 h of (a) 5Y3S (c) 5Y3A and (e) 3S3M1Y and heat-treated at 2223 K for 8 h of (b) 5Y3S (d) 5Y3A and (f) 3S3M1Y.

particularly the intergranular glassy film thickness, is an important character.[13,14] However, it is difficult to demonstrate the distribution of the very thin glassy phase between two grains by SEM. The characterization of intergranular film and the glassy pocket will be examined and reported in the near future.

3.2. Mechanical properties

Influence of microstructure on mechanical properties of β-Si_3N_4 has been well-known since 1970s.[15] The microstructure is characterized by elongated grains with high aspect ratio and a fine grain matrix (equiaxial) dispersed in glassy grain boundary phase, as shown in Fig. 8. Table 3 summarized the mechanical properties and microstructural characteristics of the as-sintered and heat-treated Si_3N_4 specimens. The high bending strength more than 700 MPa was achieved in the sintered bodies. Maximum bending strength was found up to 930 MPa in the 3S3M1Y specimen after sintering. However, bending strength decreased about 30% for the 5Y3S and 3S3M1Y specimens after the heat-treatment. Moreover, remarkable decrease in bending strength up to 60% was found in the 5Y3A specimen. One of the reasons for the decrease in bending strength after the heat-treatment may be grain growth. The increase of average grain size, as shown in Table 3, confirms the effect of heat-treatment on the decrease in bending strength. The average grain size increased three times in the 5Y3S specimen, but about twice in the 5Y3A and 3S3M1Y specimens due to the heat-treatment. Average grain size after the heat-treatment was not so large, but grain growth of columnar grains was extensive, as observed in fracture surfaces shown in Fig. 9a–f. Mechanism of higher magnitude of decrease in bending strength of the 5Y3A specimen than the other specimens is not yet clear. Young's modulus of all specimens was around 300 GPa and is similar to the commercial products, which did not so significantly change after the heat-treatment.

The effect of heat-treatment on hardness is given in Table 3. All specimens showed increase in Vickers hardness after the

Table 3
Mechanical properties and microstructure of Si_3N_4 ceramics sintered at 2123 K for 2 h and after heat-treated at 2223 K for 8 h

Properties	5Y3S		5Y3A		3S3M1Y	
	Sintered	Heat-treated	Sintered	Heat-treated	Sintered	Heat-treated
Mechanical properties						
Bending strength (MPa)	713 (36)	506 (26)	888 (90)	353 (29)	934 (53)	675 (56)
Young's modulus (GPa)	290 (1)	308 (17)	308 (8)	297 (9)	325 (10)	318 (14)
Vicker hardness (GPa)	14.9 (0.8)	20.8 (0.6)	18.3 (0.4)	21.8 (1.3)	18.8 (0.8)	21.9 (1.0)
Toughness (MPa $m^{1/2}$)	4.4 (0.2)	1.9 (0.2)	4.7 (0.2)	2.3 (0.1)	4.8 (0.1)	3.8 (0.3)
Microstructure						
Average grain size (mm)	0.4	1.2	0.4	0.9	0.4	0.8
Glassy phase (vol%)	10.0	4.8	9.5	7.0	18.5	2.4

The values in parenthesis are standard deviation.

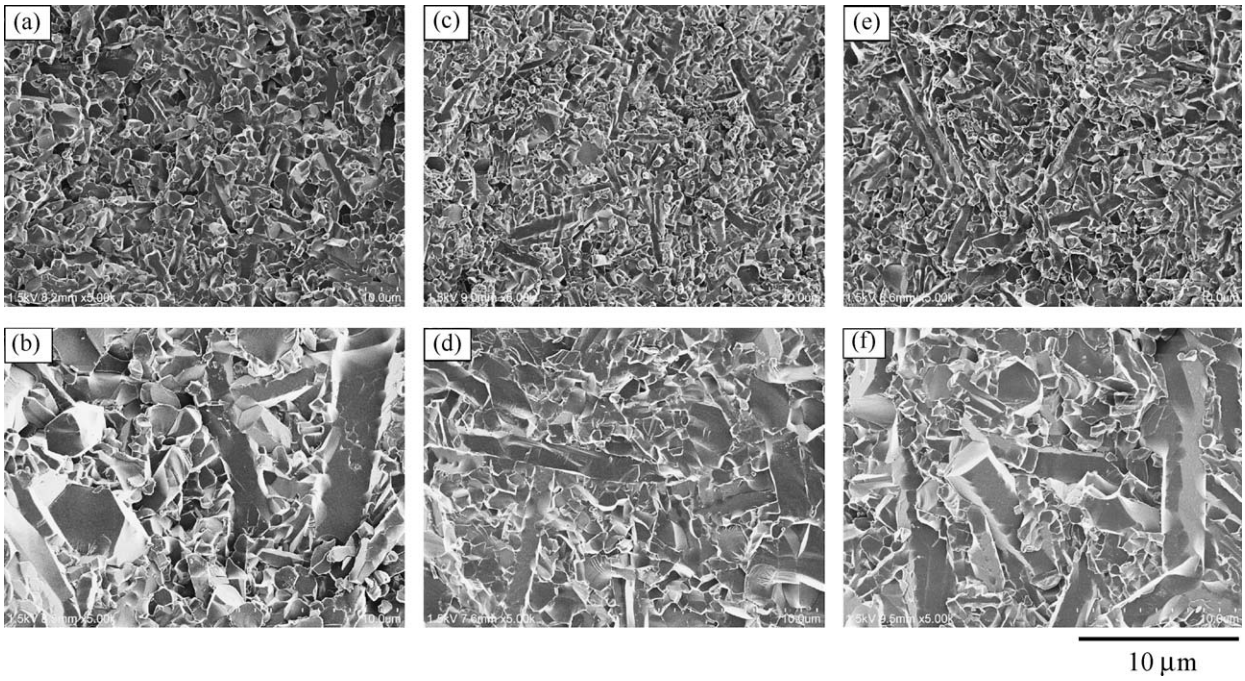

Fig. 9. SEM micrographs of fracture surface of the Si_3N_4 ceramics sintered at 2123 K for 2 h of (a) 5Y3S (c) 5Y3A and (e) 3S3M1Y and heat-treated at 2223K for 8 h of (b) 5Y3S (d) 5Y3A and (f) 3S3M1Y.

heat-treatment. The high Vickers hardness was found to be up to 19.2 GPa in the heat-treated 3S3M1Y specimen. It can be thought that the hardness increase dominated by decreasing amount of grain-boundary glassy phase[15], and not by grain growth. In the case of heat-treated 3S3M1Y specimen, the amount of glassy phase is the lowest among all specimens, as shown in Table 3.

High fracture toughness of Si_3N_4 materials in comparison with other ceramic materials is connected with the toughening mechanism, which is similar to those in whisker-reinforced composite materials, i.e. grain bridging by elongated grains and pullout. The toughening mechanism was described by presence of elongated grains and local stress between grains and intergranular glassy phase.[16] Although the fracture toughness increases with increasing volume fraction of elongated grains[17] in general cases, the fracture toughness of all specimens after the heat-treatment in this study decreased. The decrease in fracture toughness after the heat-treatment can be explained by a change in volume and composition of grain-boundary phase, particularly due to evaporation of the selective elements such as SiO or Mg during the heat-treatment. Intergranular glassy phases generally have thermal expansion coefficients higher than that of Si_3N_4 grains, then the grain-boundary phase is in under tensile stress at room temperature, i.e. specimen containing appropriate amount of grain-boundary phase shows tendency for higher fracture toughness.

The relatively higher fracture toughness (3.8 MPa $m^{1/2}$) with relatively higher strength (675 MPa) after the heat-treatment was achieved in the 3S3M1Y specimen. The highest fracture toughness within the heat-treated specimens is not explained from the amount of grain-boundary phase since it was the lowest in the case of the 3S3M1Y specimen (Table 3). The grain pullout conducted to relatively high fracture toughness of the 3S3M1Y specimen was observed as in Fig. 9f, indicating change in grain boundary phase. Further characterization is necessary to clarify the reason. Furthermore, the actual sintering condition of smaller size specimens for thermal property measurement and larger size specimens for mechanical property measurement should be somewhat different. Therefore, evaluation of thermal properties using larger specimens is set as a future work.

4. Conclusions

The heat-treatment process that was used to improve the thermal conductivity has been shown to be applicable to Si_3N_4 ceramics. The thermal conductivity, total and lattice oxygen contents and mechanical properties were evaluated for Si_3N_4 ceramics containing different additives due to the post-sintering heat-treatment at higher temperatures than sintering temperature. The following conclusions were obtained based on the results of the current work:

(1) A significant increase in thermal conductivity occurred by the post-sintering heat-treatment in the 3 mass% SiO_2, 3 mass% MgO and 1 mass% Y_2O_3 added specimen (3S3M1Y) and 5 mass% Y_2O_3 and 3 mass% SiO_2 added specimen (5Y3S) up to 85 or 89 $Wm^{-1} K^{-1}$, respectively. In both cases, the amount of total oxygen and lattice oxygen content decreased significantly.
(2) On the other hand, β-SiAlON was formed in the 5 mass% Y_2O_3 and 3 mass% Al_2O_3 added specimen (5Y3A) and the lattice oxygen of this specimen did not decrease markedly. As a result, the thermal conductivity of 5Y3A

specimen was not improved so much by the heat-treatment.

(3) In the SiO_2–MgO–Y_2O_3 added specimen, the reaction

$$Si_3N_4(s) + 3SiO_2(l) \rightarrow 6SiO(g) + 2N_2(g),$$

and

$$Si_3N_4(s) + 3MgO(s) \rightarrow 3SiO(g) + 3Mg(g) + 2N_2(g)$$

were confirmed to be progressed not only by the mass loss and the total oxygen content relationship but also by the decrease in magnesium content. The mass loss reaction is dominated by the first reaction in the initial stage, and dominated by the second reaction in the succeeding stage.

(4) Three point bending strength and fracture toughness of these Si_3N_4 ceramics decreased and Vickers hardness increased after the heat-treatment mainly by decreasing amount of grain-boundary glassy phase. Extensive grain growth of columnar grains was observed in all specimens after the heat-treatment. The relatively high fracture toughness (3.8 MPa $m^{1/2}$) with relatively high strength (675 MPa) and high hardness (19.2 GPa) were achieved after the heat-treatment in the 3S3M1Y specimen.

References

1. Watari, K. and Shinde, S. L., High thermal conductivity materials. *MRS Bull.*, 2001, **26**, 440–441.
2. Hirosaki, N., Ogata, S. and Kocer, C., Molecular dynamics calculation of the ideal thermal conductivity of single-crystal α- and β-Si_3N_4. *Phys. Rev. B*, 2002, **65**, 134110-1-11.
3. Hirao, K., Watari, K., Hayashi, H. and Kitayama, M., High thermal conductivity silicon nitride ceramic. *MRS Bull.*, 2001, **26**, 451–455.
4. Akimune, Y., Munakata, F., Matzuo, K., Hirosaki, N., Okamoto, Y. and Misono, K., Raman spectroscopic analysis of structural defects in hot isostatically pressed silicon nitride. *J. Ceram. Soc. Jpn.*, 1999, **107**, 339–342.
5. Kitayama, M., Hirao, K., Tsuge, A., Watari, K., Toriyama, M. and Kanzaki, S., Thermal conductivity of β-Si_3N_4. II. Effect of lattice oxygen. *J. Am. Ceram. Soc.*, 2000, **83**, 1985–1992.
6. Hirosaki, N., Okamoto, Y., Ando, M., Munakata, F. and Akimune, Y., Effect of grain growth on the thermal conductivity of silicon nitride. *J. Ceram. Soc. Jpn.*, 1996, **104**, 49–53.
7. Barin, I., *JANAF: Thermo Chemical Data of Pure Substances* (*1st ed.*). American Chemical Society, New York, 1989.
8. Wasanapiarnpong, T., Wada, S., Imai, M. and Yano, T., Effect of post-sintering heat-treatment on thermal conductivity of Si_3N_4 ceramics containing different additives. *J. Ceram. Soc. Jpn.*, 2005, **113**, 387–392.
9. Kitayama, M., Hirao, K., Tsuge, A., Toriyama, M. and Kanzaki, S., Oxygen content in β-Si_3N_4 crystal lattice. *J. Am. Ceram. Soc.*, 1999, **82**, 3263–3265.
10. Watari, K., Seki, Y. and Ishizaki, K., Thermal properties of HIP sintered silicon nitride. *J. Ceram. Soc. Jpn.*, 1989, **97**, 56–62.
11. Hirosaki, N., Okamoto, Y., Ando, M., Munakata, F. and Akimune, Y., Thermal conductivity of gas-pressure-sintered silicon nitride. *J. Am. Ceram. Soc.*, 1996, **79**, 2878–2882.
12. Liu, D., Chen, C. and Lee, R., Thermal diffusivity/conductivity in SiAlON ceramics. *J. Appl. Phys.*, 1995, **77**, 494–496.
13. Kleebe, H. J., Structure and chemistry of interfaces in Si_3N_4 ceramics studied by transmission electron microscopy. *J. Ceram. Soc. Jpn.*, 1997, **105**, 453–475.
14. Wang, C.-M., Pan, X., Hoffmann, M. J., Cannon, R. M. and Rühle, M., Grain boundary films in rare-earth-glass-based silicon nitride. *J. Am. Ceram. Soc.*, 1996, **79**, 788–792.
15. Riedelm, R., *Handbook of Ceramic Hard Materials*, *2*. 1st ed. Wiley-VCH, Weinheim, 2000.
16. Peterson, I. M. and Tien, T., Effect of the grain boundary thermal expansion coefficient on the fracture toughness in silicon nitride. *J. Am. Ceram. Soc.*, 1995, **78**, 2345–2352.
17. Yang, J., Sekino, T. and Niihara, K., Effect of grain growth and measurement on fracture toughness of silicon nitride ceramics. *J. Mater. Sci.*, 1999, **34**, 5543–5548.